

1 **Title:**

2 Genome-wide quantification of the effects of DNA methylation on human gene regulation

3

4 **Authors:**

5 Amanda J. Lea^{1,*}, Christopher M. Vockley^{2,3}, Rachel A. Johnston⁴, Christina A. Del Carpio⁴,
6 Luis B. Barreiro⁵, Timothy E. Reddy^{2,3,6}, Jenny Tung^{1,4,7,8,9,*}

7

8 **Affiliations:**

9 ¹Lewis-Sigler Institute for Integrative Genomics, Carl Icahn Laboratory, Washington Road,
10 Princeton University, Princeton, NJ 08544, USA

11 ²Center for Genomic and Computational Biology, Duke University Medical School, Durham,
12 North Carolina 27710, USA

13 ³Department of Biostatistics and Bioinformatics, Duke University Medical School, Durham,
14 North Carolina 27710, USA

15 ⁴Department of Evolutionary Anthropology, Duke University, Durham, North Carolina 27708,
16 USA

17 ⁵Department of Pediatrics, Sainte-Justine Hospital Research Centre, University of
18 Montreal, Montreal, Canada

19 ⁶Program in Computational Biology and Bioinformatics, Duke University, Durham, North
20 Carolina 27710, USA

21 ⁷Institute of Primate Research, National Museums of Kenya, Karen, Nairobi, Kenya

22 ⁸Duke University Population Research Institute, Duke University, Durham, North Carolina
23 27708, USA

24 ⁹Department of Biology, Duke University, Durham, North Carolina 27708, USA

25

26 *Correspondence to: Jenny Tung (jt5@duke.edu) and Amanda Lea
27 (amandalea7180@gmail.com)

28

29 **Abstract:**

30 Changes in DNA methylation are important in development and disease, but not all
31 regulatory elements act in a methylation-dependent (MD) manner. Here, we developed
32 mSTARR-seq, a high-throughput approach to quantify the effects of DNA methylation on
33 regulatory element function. We assay MD activity in 14% of the euchromatic human genome,
34 identify 2,143 MD regulatory elements, and predict MD activity using sequence and chromatin
35 state information. We identify transcription factors associated with higher activity in
36 unmethylated or methylated states, including an association between pioneer transcription factors
37 and methylated DNA. Finally, we use mSTARR-seq to predict DNA methylation-gene
38 expression correlations in primary cells. Our findings provide a map of MD regulatory activity
39 across the human genome, facilitating interpretation of the many emerging associations between
40 methylation and trait variation.

41

42

43 **Main text:**

44 DNA methylation—the covalent addition of methyl groups to nucleotide bases, most
45 often at CpG motifs—is a gene regulatory mechanism that plays a fundamental role in
46 development, disease susceptibility, and the response to environmental conditions^{1–6}. These
47 functions suggest that variation in DNA methylation should be important in explaining trait
48 variation. In support of this idea, epigenome-wide association studies (EWAS) have now
49 identified thousands of statistical relationships between phenotypic variation and DNA
50 methylation levels at individual CpG sites across the genome⁷.

51 However, not all changes in DNA methylation causally affect gene regulation^{8,9}, making
52 variation in DNA methylation more functionally important at some loci than others. Mapping
53 methylation-dependent (MD) regulatory activity across the genome is therefore essential for
54 interpreting the growing number of DNA methylation-trait associations, as well as understanding
55 the basic biology of epigenetic gene regulation. Current approaches for assaying MD activity are
56 either too low-throughput to support genome-scale analyses or have focused on measuring
57 methylation-dependent transcription factor binding outside the cellular context^{8,10–17} (Table S1).
58 These studies suggest widespread differential TF sensitivity to DNA methylation levels^{15–17}, but
59 leave open whether, and to what degree, differential sensitivity translates to differences in gene
60 expression itself.

61 To address these questions, we developed a high-throughput method, mSTARR-seq, that
62 assays the causal relationship between DNA methylation and regulatory activity within a cellular
63 context. mSTARR-seq combines genome-scale strategies for quantifying enhancer activity via
64 self-transcribing episomal reporter assays (e.g., STARR-seq¹⁸) with enzymatic manipulation of
65 DNA methylation at millions of unique CpG sites (Fig. 1). To eliminate the confounding effects
66 of DNA methylation in the vector itself, we engineered a CpG-free mSTARR-seq-specific vector
67 (*pmSTARRseq*) that also eliminates the potential for bacterial *Dam*- or *Dcm*-mediated
68 methylation (Fig. 1A). As in STARR-seq, the *pmSTARRseq* vector enables a library of query
69 fragments to be inserted in the 3' untranslated region of a constitutively expressed reporter gene,
70 such that fragments with regulatory activity drive their own transcription when transfected into a
71 cell type of interest¹⁸. Prior to transfection, the plasmid input library can be treated with either
72 the methyltransferase *M.SssI*, which methylates all CpG sites, or a sham treatment, which leaves
73 them unmethylated. The regulatory activity of fully methylated fragments can then be compared
74 to the activity of unmethylated fragments by using high-throughput sequencing to quantify their
75 relative abundances in reporter gene-derived mRNA (Fig. 1B).

76 To quantify MD activity across the human genome, we combined *MspI*-digested genomic
77 DNA (to enrich for CpG-containing fragments) with randomly sheared DNA from the HapMap
78 GM12878 cell line (Fig. 1C). We then transfected unmethylated and methylated versions of the
79 plasmid library (n=6 replicates per condition) into the K562 cell line. Forty-eight hours post-
80 transfection, we isolated and sequenced both the plasmid-derived mRNA and the fragment
81 inserts from each plasmid DNA pool (Table S2; fig. S1). We also performed bisulfite sequencing
82 on the plasmid DNA to confirm maintenance of the expected DNA methylation state throughout
83 the experiment (Fig. 1D).

84 In total, we assayed ~750,000 unique DNA fragments in each library (mean ± SD =
85 759,725 ± 252,187 fragments per replicate; one replicate from the methylated condition was
86 excluded from all analyses due to low sequencing depth), comparable to or exceeding the
87 diversity in published STARR-seq and massively parallel reporter assays (fig. S2). For
88 subsequent analysis, we binned the genome into 200 bp non-overlapping intervals and filtered

89 these regions to focus on the 277,896 intervals that overlapped at least 1 mRNA read and 1 DNA
90 read in at least half of the replicates in each condition. These 277,896 intervals were covered by
91 724,391 unique fragments of size 314 bp \pm 105 bp (mean \pm S.D.; fig. S3). This stringently
92 filtered data set represents 1.83 million unique CpG sites, 57% of fragments expected from a
93 complete *MspI* digest of the human genome, and 14% of the euchromatic genome of the K562
94 cell line (fig. S4).

95 We first focused on regions with regulatory capacity (i.e., enhancer-like activity),
96 whether in the unmethylated condition, methylated condition, or both. We identified 24,945
97 intervals of 200 bp (9% of analyzed regions, at a 10% false discovery rate) in which the
98 abundance of plasmid-derived mRNA was significantly greater than the amount of input plasmid
99 DNA (Table S3). As expected, the set of regions capable of enhancer-like activity was highly
100 enriched for K562 ENCODE chromatin states¹⁹ associated with H3K4me1 and H3K27ac, which
101 mark active enhancers (Fisher's exact test, \log_2 odds=2.53, $p < 10^{-15}$) and highly depleted in
102 regions that lacked both marks (\log_2 odds=-0.94, $p < 10^{-15}$; Fig. 2A). Regions that overlapped
103 H3K4me1 and H3K27ac-marked chromatin states also consistently displayed the largest effect
104 sizes (relative to regions that lacked these marks, or only exhibited one mark; linear model,
105 $p < 10^{-15}$; Fig. 2B). Finally, regions annotated as strong enhancers in K562 cells exhibited the
106 strongest effects of all 12 chromatin states ($p < 10^{-15}$), and contained the largest proportion of
107 elements with significant regulatory activity relative to any other chromatin state (at a 10% FDR,
108 37% of regions tested had significant activity). In general, power to detect enhancer activity
109 increased with larger query fragment sizes (Fig. 2C), suggesting that short fragments may
110 eliminate binding sites key to functional enhancer activity.

111 We next investigated which regulatory elements were functionally affected by DNA
112 methylation marks. We identified 2,143 regions with significant MD activity (8.59% of those
113 tested; 10% FDR), 88% of which were more active when unmethylated and 12% which were
114 more active when methylated (Fig. 3A; Table S4). Only 4 of the 941 CpG-free regions in the
115 analysis set (0.4%) were inferred to have MD activity, indicating a low false positive rate (Fig.
116 3B). Estimates of MD activity from mSTARR-seq were also consistent with estimates from
117 single-locus luciferase reporter assays¹³ (Fig. 1E). Overall, we found that MD enhancers have
118 higher CpG densities and contain more CpG sites than non-MD enhancers (Wilcoxon-signed
119 rank test, $W = 3.51 \times 10^7$, $p < 10^{-15}$; Fig. 3C). However, CpG density only explained 6.8% of
120 variation in the magnitude of methylation dependence, suggesting that other characteristics also
121 contribute to quantitative variation in MD activity (Spearman's $\rho = 0.246$, $p < 10^{-15}$; Fig. 3D).

122 To explore these characteristics, we used a random forests classifier to evaluate the
123 contribution of 147 genomic features to differentiating MD enhancers (specifically, the $n = 1866$
124 regions suppressed by methylation) from non-MD enhancers ($n = 5703$ regions that exceed an
125 FDR of 50% in our test for MD activity). Our feature set included information about CpG site
126 density; endogenous chromatin state, chromatin accessibility, and DNA methylation levels^{19,20};
127 evolutionary conservation²¹; and TF binding from K562 ENCODE ChIP-seq data¹⁹ (Table S5).
128 The resulting RF model predicted MD regulatory element activity with 82% accuracy (Fig. 3E).
129 In addition to CpG site information, 25 features were identified as key predictors based on two
130 measures of variable importance, the mean decrease in accuracy and the Gini coefficient
131 (FDR < 10%; Fig. 3 and Table S5). Relative to non-MD enhancers, enhancers suppressed by
132 DNA methylation were more likely to occur in regions with endogenous promoter activity and
133 less likely to occur in endogenously repressed regions of the genome. MD enhancers were also

134 more likely to contain binding sites for the TFs ELF1, E2F6, MAX, and MYC, all of which have
135 CpG sites in their canonical binding motifs (Fig. 3F).

136 Previous work indicates that many TFs are sensitive to DNA methylation levels in or near
137 their binding motifs¹⁵⁻¹⁷. This ability to “read” epigenetic modifications to DNA sequence could
138 explain, at least in part, variation in MD regulatory activity in our data set. Indeed, among the
139 1866 MD enhancers in which DNA methylation suppresses activity, we identified 24
140 significantly enriched TF binding motifs (relative to the background set of all regions with
141 mSTARR-seq regulatory activity; 1% FDR). 15 of these motifs belong to the ETS family, a 6.6x
142 enrichment over chance (hypergeometric test $p=3 \times 10^{-13}$; Fig. 4A and Table S6). ETS binding is
143 thought to be methylation dependent for ‘Class I’ ETS TFs²²⁻²⁷, which bind the canonical motif
144 ACCGGAAGT, but not for ‘Class III’ ETS family TFs, whose binding motifs do not consistently
145 include CpG sites²⁸. In support, 12 of the 15 ETS TFs we identified belong to Class I, and none
146 belong to Class III. The remaining 3 belong to Class II, for which methylation-dependent binding
147 was previously unexplored: our results suggest they behave more similarly to Class I than Class
148 III.

149 We also identified 9 significantly enriched TF binding motifs in the 257 MD enhancers
150 with increased activity in the methylated condition (1% FDR). TFs from the basic helix-loop-
151 helix (bHLH) family and GATA subfamily of zinc finger TFs were strongly enriched in this set
152 (a 2.91x and 20x enrichment over chance, hypergeometric test $p=0.33$ and $p=1.99 \times 10^{-7}$,
153 respectively; Fig. 4B and Table S7), consistent with reports that GATA3, GATA4, and bHLH
154 family TFs bind to methylated DNA outside the cellular context¹⁶. We compared our findings to
155 published chromatin accessibility data for wild type murine stem cells, which contain normal
156 patterns of DNA methylation, and triple knockouts for *DNMT1*, *DNMT3a*, and *DNMT3b*, in
157 which DNA methylation is abolished²⁹. For 5 of 10 tested GATA family TFs, open chromatin
158 regions specific to wild type (i.e., those absent in the triple knockouts) were significantly
159 enriched for their cognate binding sites (Fig. 4C), in support of the idea that GATA family TFs
160 preferentially bind methylated DNA in service of their function as “pioneer” factors³⁰. In
161 contrast, ETS family TF binding sites were almost universally (38 of 41 tested) enriched in
162 DNMT knockout-specific open chromatin regions.

163 Finally, for mSTARR-seq results to be maximally useful in interpreting DNA
164 methylation-trait associations, we reasoned that they should explain the substantial heterogeneity
165 in DNA methylation-gene expression correlations observed in real populations. To test this
166 possibility, we drew on paired DNA methylation and gene expression data for 1202 human
167 primary monocytes³¹ (a cell type closely related to K562s), in which the mean correlation
168 between DNA methylation levels and gene expression at the nearest gene is 0.006 +/- 0.189 s.d.
169 (and -0.023 +/- 0.304 for CpG sites significantly (FDR<10%) correlated with gene expression;
170 $n=81,883$ site-gene pairs). Genome-wide, we observed that significant DNA methylation-gene
171 expression correlations in monocytes (FDR<10%) were moderately enriched in mSTARR-seq
172 MD enhancers versus non-MD enhancers (Fisher’s exact test, \log_2 odds=0.60, $p=3.38 \times 10^{-4}$).
173 However, for CpG sites that display the canonical negative correlation between DNA
174 methylation and gene expression levels, this relationship was greatly strengthened (\log_2
175 odds=1.02, $p<10^{-15}$). Thus, mSTARR-seq can identify the CpG sites for which DNA methylation
176 variation is most tightly linked to gene expression variation in human primary cells.

177 Together, our findings emphasize substantial variability in the functional relationship
178 between DNA methylation and gene regulation across the genome. Using mSTARR-seq, we
179 show that the magnitude of this relationship is both predictable from genome characteristics and

180 in turn predicts *in vivo* heterogeneity in real populations. The resulting map of MD regulatory
181 activity thus provides useful guidance for prioritizing DNA methylation-trait associations for
182 further investigation: CpG sites in which DNA methylation levels causally influence gene
183 expression are more likely to be of interest than those that are effectively silent. In addition, we
184 provide support for the hypothesis that pioneer TFs, such as members of the GATA TF family,
185 have a higher affinity for methylated DNA, potentially aiding in their ability to bind condensed
186 chromatin³⁰. Indeed, in addition to GATA family TFs, TFs important in development and cell
187 fate, such as FOXA, MyoD, and TCF21, are enriched among MD enhancers with increased
188 activity when methylated. These results raise the interesting possibility that preferential binding
189 of methylated loci could be used to aid in pioneer TF discovery. Finally, mSTARR-seq can be
190 applied as an efficient, high-throughput strategy to map MD activity in a variety of settings,
191 including at specific loci of interest, across cell types, or across cellular environments.
192 Epigenome editing approaches will be useful for following up the most interesting loci.

193
194

195 **ACKNOWLEDGMENTS**

196 We thank Michael Yuan and members of the Reddy and Tung labs for experimental
197 contributions and helpful discussions, and the Rehli lab for the gift of the pCpGL vector. This
198 work was supported by a Sloan Foundation Early Career Research Fellowship, NIH grants R01-
199 GM102562 and R21-AG049936, and NSF grant BCS-1455808. RNA-seq and DNA-seq data
200 will be deposited in NCBI's Short Read Archive following publication. Code and data will be
201 available at https://github.com/AmandaJLea/mstarr_seq following publication. The mSTARR-
202 seq protocol is available online at www.tung-lab.org/protocols-and-software.html. The
203 *pmSTARRseq* vector and DNA input library used in the experiments described here (fig. S5) can
204 be shared with interested third parties pending a mutual transfer and non-commercial use
205 agreement (see details at www.tung-lab.org/protocols-and-software.html).

206
207
208

209 **FIGURE LEGENDS**

210
211 **Figure 1. mSTARR-seq experimental design.** (A) The *pmSTARRseq* vector is entirely CpG
212 free. It is designed so that functional regulatory elements will self-transcribe to produce a fully
213 processed mRNA transcript, including a transcribed region (dark blue) that spans a synthetic
214 intron (teal), the sequence of the regulatory element itself (green), and an SV40 polyA signal
215 (orange). (B) DNA fragments are cloned into *pmSTARRseq* in high-throughput. The resulting
216 library is subjected to either experimental methylation (*M.SssI* treatment) or a sham treatment,
217 and each pool is transfected into a cell line of interest (here, we used the K562 myeloid cell line;
218 n=6 replicates per condition). After a 48 hr incubation period, plasmid DNA and plasmid-derived
219 mRNA are extracted and the variable insert regions sequenced. (C) As input, we used GM12878
220 DNA fragmented through random shearing or *MspI* digest (to enrich for CpG-containing regions
221 of the genome). The resulting fragment pools were mixed in a 2:1 ratio. (D) Bisulfite sequencing
222 of the GM12878 plasmid pool pre- and post-transfection confirms that *M.SssI* treatment almost
223 completely methylates CpG sites contained in the candidate regulatory elements. High
224 methylation levels are maintained throughout the experiment. Y-axis shows mean CpG
225 methylation level per experimental replicate. (E) Low-throughput validation (CpG-free luciferase
226 reporter assay¹²) of three candidate regulatory elements with no (FDR>0.2), weak
227 (0.05<FDR<0.1), or strong evidence (FDR<0.001) for MD activity in mSTARR-seq (Wilcoxon
228 p-value, comparison between conditions: 0.069, 1.55×10^{-4} , and 1.55×10^{-4} , respectively).

229
230 **Figure 2. mSTARR-seq identifies regions with endogenous regulatory activity.** (A) Regions
231 with significant regulatory activity in the mSTARR-seq assay are enriched for chromatin state
232 annotations defined by active marks (H3K4me1 and H3K27ac, colored orange). The y-axis
233 depicts the $\log_2(\text{odds})$ from a two-sided Fisher's exact test for enrichment (or depletion) of
234 mSTARR-seq identified enhancers in each of the 12 annotated chromatin states in K562 cells
235 ($p < 0.05$ for all tests). Positive y-axis values indicate enrichment and negative values indicate
236 depletion. (B) Effect sizes for loci with significant enhancer activity (FDR<10%; x-axis) are
237 consistently larger for mSTARR-seq identified enhancers that occur in chromatin state
238 annotations defined by active marks. (C) Binning regions with significant mSTARR-seq
239 enhancer activity by fragment length reveals that larger fragments are more strongly enriched for
240 ENCODE-annotated 'strong enhancers'. The y-axis depicts the $\log_2(\text{odds})$ from a Fisher's exact
241 test for enrichment of mSTARR-seq enhancers (binned by deciles of fragment length) in either
242 of the two 'strong enhancer' chromatin states ($p < 0.05$ for all tests).

243
244 **Figure 3. mSTARR-seq identification and prediction of MD enhancers.** (A) The distribution
245 of differences in normalized mRNA transcript abundance between the unmethylated and
246 methylated conditions (all significant MD enhancers are shown). (B) CpG-free MD enhancers
247 occur at a 20.2-fold lower rate than CpG-free windows with no MD enhancer activity. (C)
248 Distribution of fragment CpG density for regions identified as MD versus non-MD enhancers.
249 (D) CpG-dense mSTARR-seq enhancers tend to be repressed by DNA methylation, such that
250 mRNA abundance is higher in the unmethylated condition relative to the methylated condition
251 (positive y-axis value). X-axis: CpG sites/fragment window length (Spearman's rho for
252 correlation between x and y axes=0.246, $p < 10^{-15}$; n=24,945 regions with significant regulatory
253 element activity). (E) The proportion of non-MD and MD enhancers that were accurately
254 classified via a random forests (RF) classifier. (F) Features that distinguish MD and non-MD
255 enhancers in the RF classifier (10% FDR). X-axis: mean decrease in predictive accuracy when

256 excluding the focal variable. Blue: positive prediction of non-MD enhancers; white: positive
257 prediction of MD enhancers.

258

259 **Figure 4. mSTARR-seq identifies MD-dependent transcription factor-DNA binding.** (A)

260 Transcription factor motifs that are enriched in MD enhancers that are more active when

261 unmethylated, colored by TF family. (B) TF motifs that are enriched in MD enhancers that are

262 more active when methylated. (C) DNase hypersensitive sites (DHS) specific to murine stem

263 cells that lack DNA methylation (DNMT triple knock-outs: TKO) are strongly enriched for ETS

264 family binding sites relative to wild type cells with intact DNA methylation. In contrast, DHSs

265 specific to wild type cells are enriched for GATA family binding sites relative to triple knock-

266 outs. DHS data are from²⁵. X-axis: percent of knockout-specific DHSs that contain a given TF

267 binding motif (n=1251 motifs). Y-axis: Ratio of knockout versus wild-type specific DHSs

268 containing a given TF binding site motif. Colored dots circled in black show significant

269 enrichment for a ETS or GATA family TF (10% FDR in a hypogeometric test).

270

271

272

273 **SUPPLEMENTARY MATERIALS**

274 **Author Contributions**

275 **Materials and Methods**

276 *Laboratory techniques and methods*

277 Text S1. pmSTARRseq design

278 Text S2. Generation of plasmid libraries for mSTARR-seq

279 Text S3. Cell culture, plasmid transfection, and cell harvesting

280 Text S4. Isolation and preparation of mRNA derived from the mSTARR-seq plasmid

281 Text S5. Preparation of plasmid DNA for DNA-seq and bisulfite sequencing

282 Text S6. Luciferase reporter assays

283 *Computational techniques and methods*

284 Text S7. Low-level data processing

285 Text S8. Identification of enhancers and methylation dependent (MD) enhancers

286 Text S9. Annotation of analyzed mSTARR-seq fragments

287 Text S10. *In silico* *MspI* digest

288 Text S11. Random forests classification

289 Text S12. Transcription factor binding motif enrichment analyses

290 Text S13. Correlations between DNA methylation and gene expression levels in primary

291 cells

292 **Figures S1-S5**

293 Figure S1. Diversity in plasmid DNA-seq libraries versus mRNA-seq libraries.

294 Figure S2. Fragment diversity in mSTARR-seq experiments versus other published
295 multiplexed reporter assays (MPRA) or STARR-seq experiments.

296 Figure S3. Distribution of analyzed fragment lengths.

297 Figure S4. Regions covered by mSTARR-seq.

298 Figure S5. Retransforming a plasmid pool results in almost no loss in diversity.

299 **Tables S1-S8**

300 Table S1: Other methods for testing the causal relationship between DNA methylation
301 and gene regulation.

302 Table S2: Samples sequenced in this study.

303 Table S3: Linear model results testing for mSTARR-seq regulatory activity.

304 Table S4: Linear model results testing for methylation-dependent regulatory activity.

305 Table S5: Random forests analysis results.

306 Table S6: TF motif enrichment results for MD enhancers with greater activity in the
307 unmethylated condition.

308 Table S7: TF motif enrichment results for MD enhancers with greater activity in the
309 methylated condition.

310 Table S8A: Luciferase reporter assay details.

311 Table S8B: Luciferase reporter assay results.

312

313

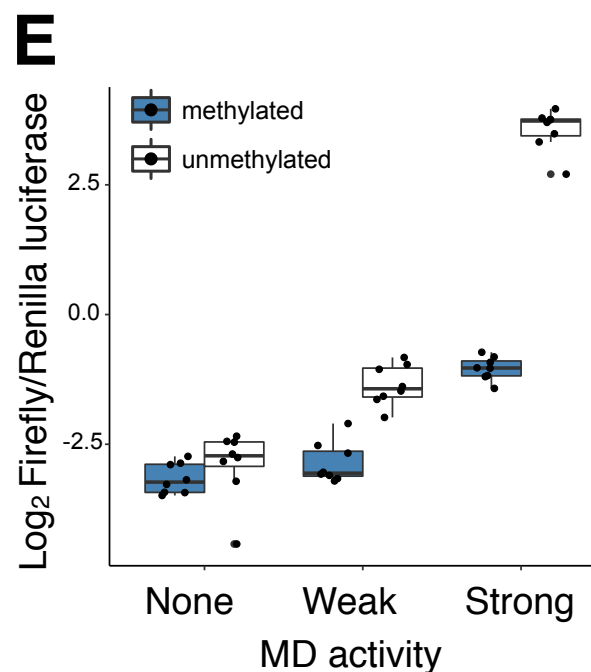
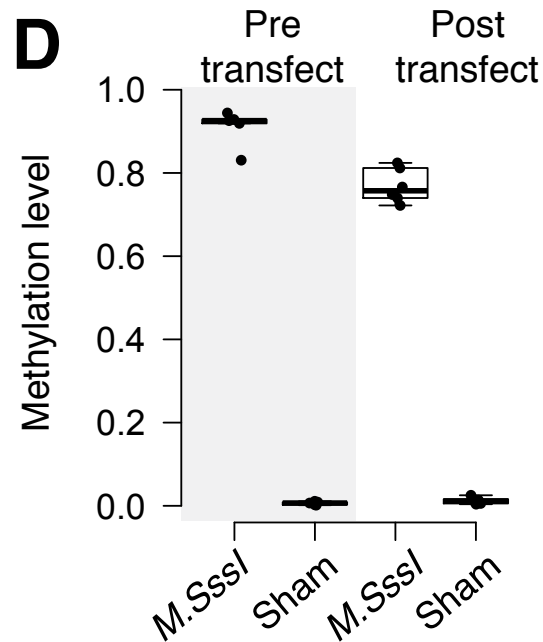
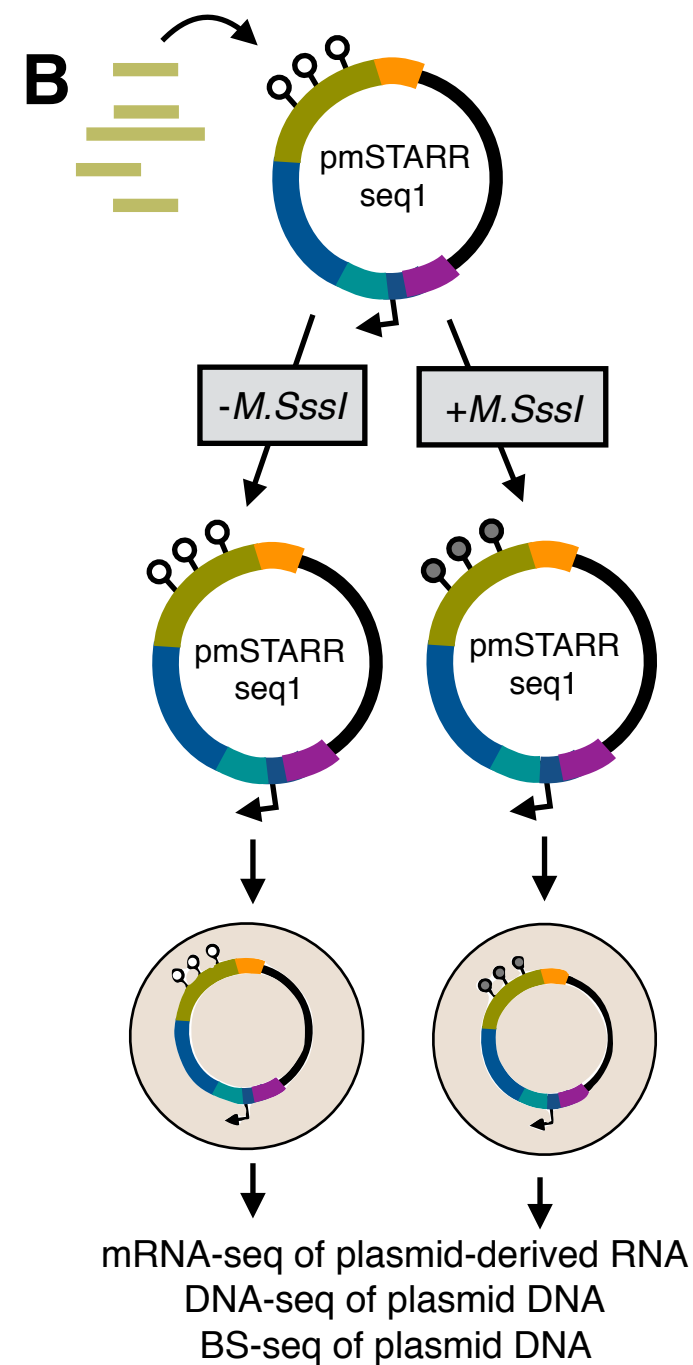
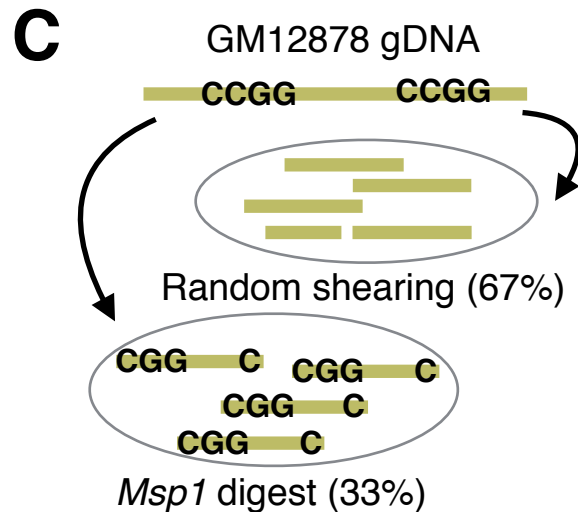
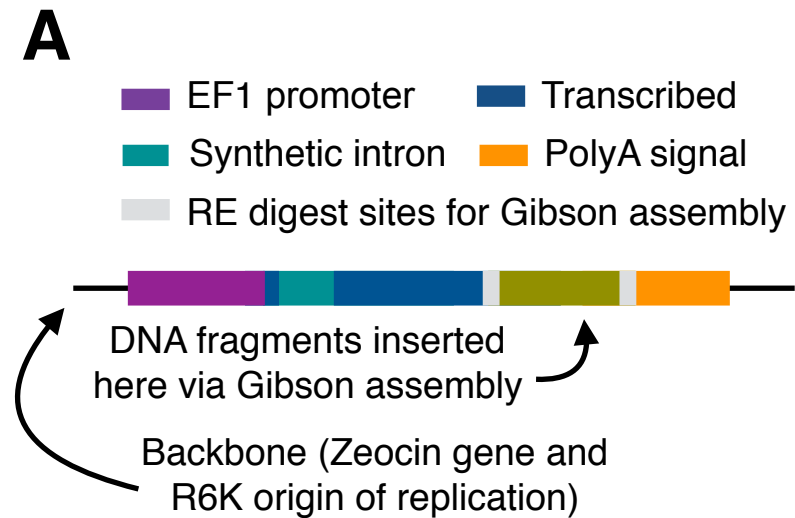
314

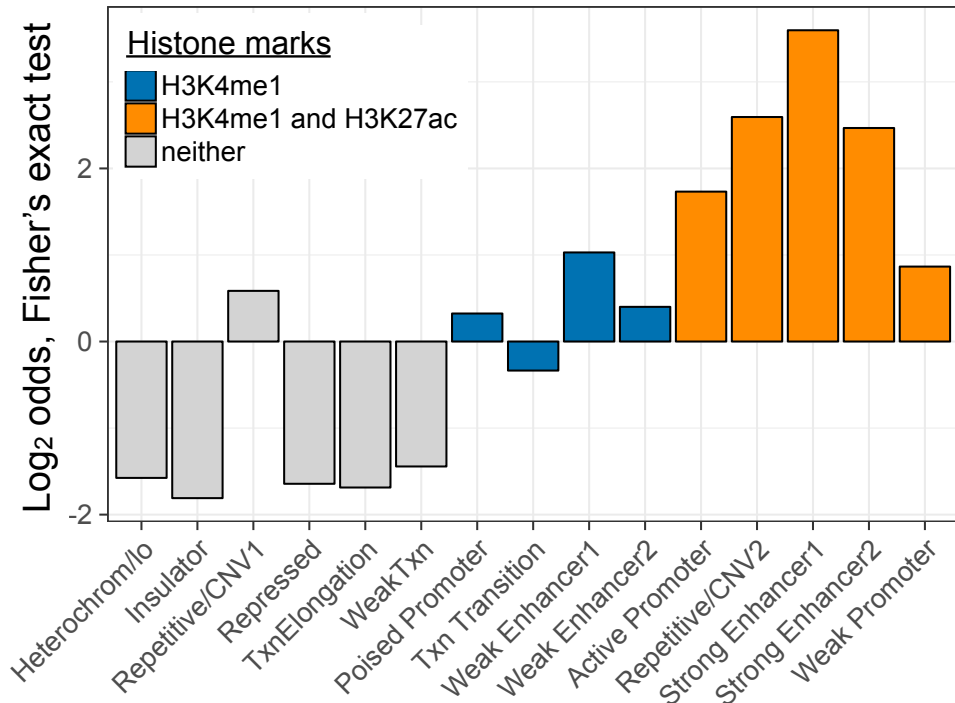
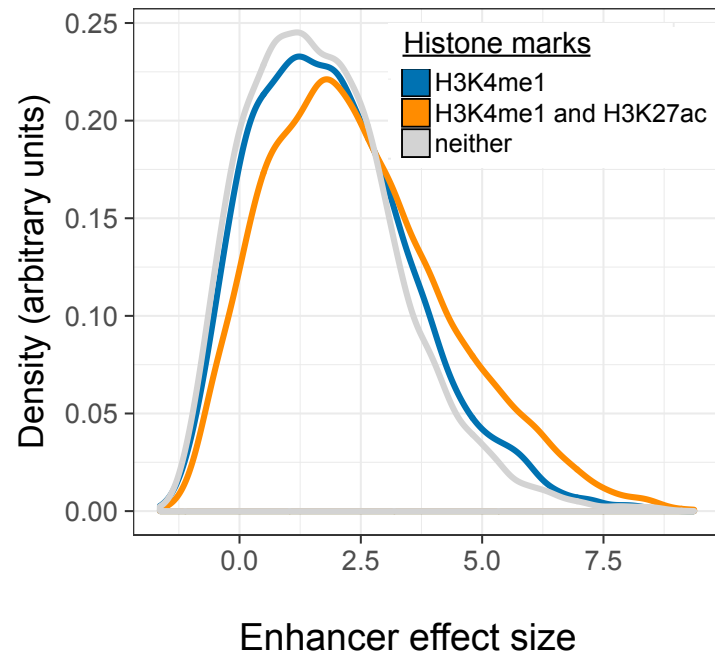
315 **REFERENCES AND NOTES**

316

- 317 1. Smith, Z. D. & Meissner, A. DNA methylation: roles in mammalian development. *Nat.*
318 *Rev. Genet.* **14**, 204–220 (2013).
- 319 2. Heyn, H. & Esteller, M. DNA methylation profiling in the clinic: applications and
320 challenges. *Nat. Rev. Genet.* **13**, 679–92 (2012).
- 321 3. El-Maarri, O. DNA methylation and human disease. *Nat. Rev. Genet.* **544**, 135–144
322 (2005).
- 323 4. Feil, R. & Fraga, M. F. Epigenetics and the environment: emerging patterns and
324 implications. *Nat. Rev. Genet.* **13**, 97–109 (2011).
- 325 5. Jirtle, R. L. & Skinner, M. K. Environmental epigenomics and disease susceptibility. *Nat.*
326 *Rev. Genet.* **8**, 253–62 (2007).
- 327 6. Jaenisch, R. & Bird, A. Epigenetic regulation of gene expression: how the genome
328 integrates intrinsic and environmental signals. *Nat. Genet.* **33 Suppl**, 245–54 (2003).
- 329 7. Rakyan, V. K., Down, T. a, Balding, D. J. & Beck, S. Epigenome-wide association studies
330 for common human diseases. *Nat. Rev. Genet.* **12**, 529–41 (2011).
- 331 8. Maeder, M. L. *et al.* Targeted DNA demethylation and activation of endogenous genes
332 using programmable TALE-TET1 fusion proteins. *Nat. Biotechnol.* **31**, 1137–42 (2013).
- 333 9. Andersson, R. *et al.* An atlas of active enhancers across human cell types and tissues.
334 *Nature* **507**, 455–61 (2014).
- 335 10. Christman, J. K. 5-Azacytidine and 5-aza-2'-deoxycytidine as inhibitors of DNA
336 methylation: mechanistic studies and their implications for cancer therapy. *Oncogene* **21**,
337 5483–5495 (2002).
- 338 11. Liu, X. S. *et al.* Editing DNA Methylation in the Mammalian Genome. *Cell* **167**, 233–
339 247.e17 (2016).
- 340 12. Rivenbark, A. G. *et al.* Epigenetic reprogramming of cancer cells via targeted DNA
341 methylation. *Epigenetics* **7**, 350–60 (2012).
- 342 13. Klug, M. & Rehli, M. Functional Analysis of Promoter CpG Methylation Using a CpG-
343 Free Luciferase Reporter Vector. *Epigenetics* **1**, 127–130 (2006).
- 344 14. Mann, I. K. *et al.* CG methylated microarrays identify a novel methylated sequence bound
345 by the CEBPB | ATF4 heterodimer that is active in vivo. *Genome Res.* 988–997 (2013).
346 doi:10.1101/gr.146654.112
- 347 15. O'Malley, R. C. *et al.* Cistrome and Epicistrome Features Shape the Regulatory DNA
348 Landscape. *Cell* **165**, 1280–1292 (2016).
- 349 16. Hu, S. *et al.* DNA methylation presents distinct binding sites for human transcription
350 factors. *eLife* **2013**, 1–16 (2013).
- 351 17. Yin, Y. *et al.* Impact of cytosine methylation on DNA binding specificities of human
352 transcription factors. *Science* **356**, eaaj2239 (2017).
- 353 18. Arnold, C. D. *et al.* Genome-wide quantitative enhancer activity maps identified by
354 STARR-seq. *Science* **339**, 1074–1077 (2013).
- 355 19. Dunham, I. *et al.* An integrated encyclopedia of DNA elements in the human genome.
356 *Nature* **489**, 57–74 (2012).
- 357 20. Roadmap Epigenomics Consortium *et al.* Integrative analysis of 111 reference human
358 epigenomes. *Nature* **518**, 317–330 (2015).
- 359 21. Spieth, J., Hillier, L. W. & Wilson, R. K. Evolutionarily conserved elements in vertebrate,
360 insect, worm, and yeast genomes. *Genome Res.* **15**, 1034–1050 (2005).

- 361 22. Stephens, D. C. & Poon, G. M. K. Differential sensitivity to methylated DNA by ETS-
362 family transcription factors is intrinsically encoded in their DNA-binding domains.
363 *Nucleic Acids Res.* **44**, 8671–8681 (2016).
- 364 23. Yokomori, N., Kobayashi, R., Moore, R., Sueyoshi, T. & Negishi, M. A DNA methylation
365 site in the male-specific P450 (Cyp 2d-9) promoter and binding of the heteromeric
366 transcription factor GABP. *Mol. Cell. Biol.* **15**, 5355–5362 (1995).
- 367 24. Umezawa, A. *et al.* Methylation of an ETS site in the intron enhancer of the keratin 18
368 gene participates in tissue-specific repression. *Mol. Cell. Biol.* **17**, 4885–94 (1997).
- 369 25. Lucas, M. E., Crider, K. S., Powell, D. R., Kapoor-Vazirani, P. & Vertino, P. M.
370 Methylation-sensitive regulation of TMS1/ASC by the Ets factor, GA-binding protein. *J.*
371 *Biol. Chem.* **284**, 14698–14709 (2009).
- 372 26. Polansky, J. K. *et al.* Methylation matters: Binding of Ets-1 to the demethylated Foxp3
373 gene contributes to the stabilization of Foxp3 expression in regulatory T cells. *J. Mol.*
374 *Med.* **88**, 1029–1040 (2010).
- 375 27. Cooper, C. D. O., Newman, J. A., Aitkenhead, H., Allerston, C. K. & Gileadi, O.
376 Structures of the Ets protein DNA-binding domains of transcription factors Etv1, Etv4,
377 Etv5, and Fev: Determinants of DNA binding and redox regulation by disulfide bond
378 formation. *J. Biol. Chem.* **290**, 13692–13709 (2015).
- 379 28. Wei, G.-H. *et al.* Genome-wide analysis of ETS-family DNA-binding in vitro and in vivo.
380 *EMBO J.* **29**, 2147–60 (2010).
- 381 29. Domcke, S. *et al.* Competition between DNA methylation and transcription factors
382 determines binding of NRF1. *Nature* **528**, 575–579 (2015).
- 383 30. Zhu, H., Wang, G. & Qian, J. Transcription factors as readers and effectors of DNA
384 methylation. *Nat. Rev. Genet.* **17**, 551–65 (2016).
- 385 31. Reynolds, L. M. *et al.* Age-related variations in the methylome associated with gene
386 expression in human monocytes and T cells. *Nat. Commun.* **5**, 5366 (2014).
387
388



A**B****C**